23rd International North Sea Flow Measurement Workshop
Tønsberg, Norway, 18 - 21 October 2005

LIQUID ULTRASONIC FLOW METERS FOR CRUDE OIL MEASUREMENT

Raymond J. Kalivoda, FMC Measurement Solutions, 1602 Wagner Avenue, Box 10428 Erie, Pennsylvania, U.S.A.
Per Lunde, Christian Michelsen Research AS (CMR), Box 6031 Postterminalen, N-5892 Bergen, Norway.

ABSTRACT

Liquid ultrasonic flow meters (LUFMs) are gaining popularity for the accurate measurement of petroleum products. In North America the first edition of the API standard "Measurement of liquid hydrocarbons by ultrasonic flow meters using transit time technology" was issued in February 2005. It addresses both refined petroleum products and crude oil applications. Its field of application is mainly custody transfer applications but it does provide general guidelines for the installation and operation of LUFM's other applications such as allocation, check meters and leak detection.

As with all new technologies performance claims are at times exaggerated or misunderstood and application knowledge is limited. Since ultrasonic meters have no moving parts they appear to have fewer limitations than other liquid flow meters. Liquids ultrasonic flow meters, like turbine meters, are sensitive to fluid properties. It is increasingly more difficult to apply on high viscosity products then on lighter hydrocarbon products. Therefore application data or experience on the measurement of refined or light crude oil may not necessarily be transferred to measuring medium to heavy crude oils. Before better and more quantitative knowledge is available on how LUFMs react on different fluids, the arguments advocating reduced need for in-situ proving and increased dependency on laboratory flow calibration (e.g. using water instead of hydrocarbons) may be questionable.

The present paper explores the accurate measurement of crude oil with liquid ultrasonic meters. It defines the unique characteristics of the different API grades of crude oils and how they can affect the accuracy of the liquid ultrasonic measurement. Flow testing results using a new LUFM design are discussed. The paper is intended to provide increased insight into the potentials and limitations of crude oil measurement using ultrasonic flow meters.

1. INTRODUCTION

Because of their non-intrusive design features, there is much excitement today about extending the application of liquid ultrasonic meters (LUFMs) to a wider range of crude oil measurement. They have been used in the petroleum industry for many years in non-custody transfer applications such as leak detection, allocation measurement and check meter measurement. With advancements in multiprocessors, transducers and electronic technology, multipath ultrasonic flow meters are now available with higher levels of accuracy. They are recognized in many European countries for custody transfer service and recently in North America with publication of the API Standard *Measurement of Liquid Hydrocarbons by Ultrasonic Flowmeters Using Transit Time Technology* [1]. Most of the applications, though, have been on refined products or light to medium crude oils.

Crude oil measurement defines a wide range of applications from light condensates with a viscosity of less than 0.5 cP to heavy crude oils with less that 10 API gravity, over 2000 cP. Ultrasonic meters infer the volumetric through-put by measuring the velocity over the flow area. As all velocity meters they are Reynolds Number depended, that is, they are more or less

affected by the relationship between velocity and viscosity. They may also be affected by entrained solids, gases, waxes and chemicals contained in the crude oil, which further complicates their application on crude oils

The present paper explores ultrasonic meter technology and its application on crude oils. In Sections 2 and 3 the LUFM principles and some crude oil characteristics are reviewed briefly, as a reference for the paper. Various influences of fluid properties on the LUFM metering principle are discussed in Section 4, as a background to understand how the LUFM may react on different fluids. Proving issues of the LUFM are then addressed in Section 5. Test results for a novel type of LUFM are presented in Section 6, with conclusions given at the end (Section 7).

2. LUFM PRINCIPLES

In ultrasonic transit time flow meters (UFM) the flow direction, the flow velocity and the sound velocity of the fluid are estimated from the measured up- and downstream transit times. These transit times are obtained by transmitting and detecting acoustic pulses up- and downstream with respect to the direction of the flow, using ultrasonic transducers and dedicated electronics. One or several acoustic paths may be used, depending on the accuracy required. For further details, cf. e.g. [1-6]. Fig. 1 shows a cross-section of such a meter, schematically.

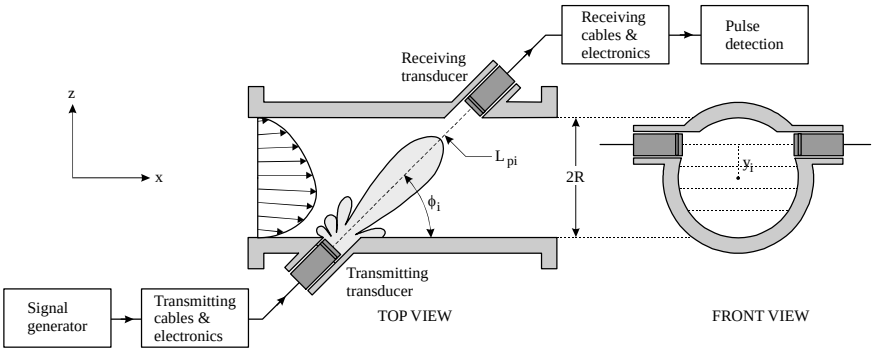

Fig. 1. Schematic illustration of a single path in a multipath ultrasonic transit time flow meter with non-reflecting paths (for downstream sound propagation). (Left: centre path example (y_i = 0); Right: path at lateral chord position y_i.)

In UFMs with reflecting or non-reflecting paths, the volumetric flow rate (at line conditions) is given as [1-6]

$$q_{UFM} = \pi R^2 \bar{v}_A, \qquad \bar{v}_A = \sum_{i=1}^{N} w_i \bar{v}_i, \qquad \bar{v}_i = (N_{refl,i} + 1) \frac{2\sqrt{R^2 - y_i^2}\,(t_{1i} - t_{2i})}{t_{1i} t_{2i} |\sin 2\phi_i|},$$

(1)

where (cf. Fig. 1) R is the inner radius of the UFM meter body; $\bar{v}_A$ is the axial volume flow velocity (at line conditions); N is the number of acoustic paths; i is the path number; w_i is the integration weight factor for path no. i; $\bar{v}_i$ is the average axial flow velocity along path no. i (i.e. the line integral along the path); y_i is the lateral distance from the pipe center (lateral chord position) for path no. i; L_i is the interrogation length for path no. i; ϕ_i is the inclination angle (relative to the pipe axis) of path no. i; t_{1i} and t_{2i} are the measured transit times for upstream and

downstream sound propagation of path no. i; and $N_{refl,i}$ is the number of wall reflections for path no. i ($N_{refl,i}$ = 0, 1 or 2 in current UFMs), i = 1, …, N.

3. CRUDE OIL CHARACTERISTICS IMPORTANT TO LUFM PERFORMANCE

Crude oil characteristics are important to the measurement of crude oil. Viscosity is of primary importance in determining the feasibility and accuracy of measurement with an ultrasonic meter. But also important are entrained gas, water, solids, wax, and corrosive chemicals. These characteristics are defined in Crude Oil Assays[1] and include:

- **API gravity**. Crude oils are normally defined by their API gravity. The definition of API gravity is the density of crude oil at a specific temperature compared to the density of water at a standard temperature, 60 F. The relationship between specific gravity (SG) and API gravity is:

$$\text{SG (60F/60F)} = 141.5 / (131.5 + \text{API}) \quad (2)$$

  API gravity is also loosely related to viscosity. In general as the API number decreases the viscosity increases. Crude oils vary widely from the different production fields, but can be divided by API gravity into four ranges as shown in Table 1.

Table 1. API gravity of condensates and crude oils.

Petroleum Liquids	API Gravity Range	Viscosity [cSt]
Condensate	< 50	0.5 – 0.8
Light crude	35 – 50	< 1 – 20
Medium crude	25 – 34	20 – 500
Heavy crude	< 10 to 24	100 - >2000

  For light crude oils there is a fairly close relation between viscosity and API gravity. But for medium crude oils and heavy crude oils it is important to obtain the viscosity from the assay or from specific tests.

- **Viscosity** can be expressed in many different units. For the petroleum industry the most commonly used viscosity units are:

  - Kinematic Viscosity (symbolically, v), has units of Stokes (St). It is, for our purposes the most suitable viscosity to use. In the metric system the kinematic viscosity unit is cm^2/s (centimeter^2/second). As the value of Kinematic Viscosity is normally small, the unit is often converted by multiplying by 100 and calling the unit centistokes (cSt).
  - Saybolt Universal Viscosity (SSU). SSU can be converted to cSt using a conversation table.
  - Dynamic Viscosity (symbolically, μ), has units of Poise (P). Poise can be converted to Stokes by dividing by the specific gravity, i.e. St = P / SG. In the metric system,

[1] The Hydrocarbon Measurement Committee (HMC) has assays of a wide range of crude oils. This information can be found online at: http://www.melvcon.co.uk/Crude_Oil_Data/crude_oil_data.html. This website is operated on behalf of the UK Energy Institute HMC-4 Oil Transportation Measurement Committees to provide rapid access to crude oil measurement and property data. The data is submitted by major oil companies listed on the site.

the dynamic viscosity unit is Pa·s (Pascal·second). Like Kinematic Viscosity, the Poise is often multiplied by 100 and named centipoise (cP).

The viscosity of all liquids varies with temperature. Table 2 illustrates the effect of temperature on the viscosity of selected products. In absolute terms the more viscous the product the greater temperature affects the viscosity. It is important when evaluating any meter application that the viscosity of each product must be specified over the operating temperature range.

Table 2. Effect of temperature on the viscosity of selected products.

API gravity	**Viscosity in cP @ deg F (deg C)**		
for selective crude oils	**60 (15)**	**100 (38)**	**150 (66)**
48 API	2.7	1.7	1.1
32.6 API	21	9	5
25.3 API	1442	243	93
17.8 API	-	340	-
16.2 API	-	574	-
10 API	-	1294	-

- **Cloud-Point** in a petroleum product is the temperature at which wax crystals begin to form as it is cooled. If a meter is operated below the cloud point, wax can form on the measurement element, which can notably affect the meter's accuracy. Some meters are considerably more tolerant of waxing than other meters. For example, after an initial build-up of wax on the walls of a Smith PD, the rotating blades wipe the surfaces, and the meter factor remains stable. In the case of velocity meters (eg: ultrasonic, turbine) there is a continuous meter factor shift as the wax builds-up.

- **Sediment and Water (S&W).** This is a collective term for non-hydrocarbons found in crude oil. In API MPMS Chapter 1, S&W is defined as "A material, coexisting with yet foreign to a petroleum liquid,… may include free water and sediment (FW&S) and emulsified or suspended water and sediment (SW&S)." Since all pipelines regulate the amount of S&W they will accept, normally less than 1%, a crude oil within these requirements is termed "pipeline quality oil". In general "pipeline quality oil" may not be a problem for measurement with an ultrasonic meter. Crude oil at the production lever and in gathering lines may be a problem, so the characteristics of these crude oils must be carefully considered before making a decision on the type of meter to use.

- **Gases.** Slugs or entrained gas will not damage an ultrasonic meter but it can adversely affect the measurement accuracy. Even a small number of gas bubbles can cause attenuation of the ultrasonic signal. The degree of attenuation depends on a number of factors such as e.g. pressure, bubble size, amount of free gas, signal frequency, etc. (cf. Section 4.1).

- **Chemical Contaminants.** As with S&W, pipelines have strict limits on the type and amounts of chemicals in the crude oils they will transport. Normally "pipeline quality oil" is not a problem. Crude oils at the production level can have a variety of chemicals and it is important to check the compatibility of the meters materials of construction with the crude oil assay.

4. SENSITIVITY OF LUFMs TO FLUID PROPERTIES

Inherent benefits of liquid ultrasonic flow meters include no moving parts, "no" wear (as compared to e.g. turbines and PD meters), low pressure drop, wide rangeability, and potentials of low maintenance. This does not mean that such meters cannot fail, however, or be subject to gradually or abrupt degraded performance. Such factors have been discussed e.g. in [10]. Diagnostic tools are available in present-day LUFMs which in many cases are able to alarm the user in case of degraded performance.

Another important factor, which becomes relevant e.g. when transforming measurement results from one type of fluid to another and different fluid (such as e.g. by flow calibration the meter in a water laboratory facility, for long-time field operation on oil products [10,11]), is the influence of fluid properties on the meter. On a qualitative (overall) level, many of the influences of fluid properties are known, and have been addressed by various authors. However, on a *quantitative* level, the knowledge on such influences is definitely insufficient today, and any contribution to close this knowledge gap should be welcome. The following discussion may represent a contribution to the process of filling in on some parts of this knowledge gap.

The influence of fluid properties on the UFM performance may be classified in two main groups, according to *how* they influence on the UFM:

(a) Signal quality; i.e. the signal attenuation and signal-to-noise ratio (SNR) in the acoustic paths,
(b) Flow profiles and integration mehod; i.e. how the numerical integration method used to combine the individual acoustic path measurements into a full volumetric flow rate measurement, handles different flow velocity profiles met in practice.

These topics are discussed in the following.

4.1. Signal quality: Sound attenuation and SNR

The signal strength, or more precisely, the signal-to-noise ratio (SNR), is crucial for the accuracy of the transit time measurements made in the UFM. Reduced SNR means higher uncertainty of the transit time measurement, and thereby higher uncertainty of the volumetric flow rate measurement.

Noise is classified as coherent noise (signal interference) and incoherent noise ("signals" with random phase relative to the measurement signal). Coherent noise contributions may be e.g. (a) transducer "ringing" effects, (b) spoolpiece borne signals (acoustic cross talk), (c) liquid borne reflections (transducer ports reflections, pipe wall reflections/reverberation), etc. Incoherent noise contributions may be e.g. (a) electromagnetic noise (RFI), (b) flow noise, (c) valve noise, (d) structural (pipe) vibrations, etc.

The "strength" (amplitude) of the measurement signal has to "compete" with such noise contributions, to give a sufficient SNR. To illustrate this situation, SNR requirements[2] for an example of a "standard" zero crossing time detection method is given in Table 3, for incoherent

[2] The example requirements of Table 1 apply to the processed signals on which the time detection is made.

and coherent noise contributions, respectively, and for different pipe dimensions (6" - 20" LUFMs).

Table 3. Signal-to-noise (SNR) requirements for an example of a "standard" zero crossing time detection method, in an ultrasonic liquid flow meter (LUFM) for precision custody transfer measurement.

	Pipe diameter		
	6”	**12”**	**20”**
Incoherent noise	> 45 dB	> 40 dB	> 35 dB
Coherent noise (“worst case”)	> 65 dB	> 60 dB	> 55 dB

It is noted that for single-phase water (with its relatively low viscosity), the 6" and 20" requirements of Table 3 are about "equivalent", since the geometrical attenuation increases about 10 dB from 6" to 20" LUFMs. In viscous oil, however, and in cases with water and/or gas contents, etc., the 20" requirements may be the strongest.

A number of fluid-dependent factors may contribute to attenuate the measurement signal, thereby decreasing the SNR. The sound attenuation coefficient, α, consists of a number of contributions, such as e.g.

$$\alpha = \alpha_{abs} + \alpha_{wio} + \alpha_{gas} + \alpha_{solids} + \alpha_{wax}\,, \tag{3}$$

where α_{abs} is the sound absorption coefficient (due to shear viscosity, bulk viscosity, thermal conductivity and possible relaxation effects), and α_{wio}, α_{gas}, α_{solids} and α_{wax} account for excess attenuation due to water contents, gas contents, solid particles (e.g. wax), and contamination (wax) at transducers, respectively.

The properties of the fluid under measurement may influence significantly on the signal attenuation, and thus on the SNR and the time detection accuracy. Broadly speaking, sound attenuation below about 0.1 dB/cm may not influence much on the meter performance, except for large meters. For 6" and 20" meters, this figure would correspond to about 2 dB and 7 dB increased attenuation, respectively, for centre paths. Various effects contributing to the sound attenuation are discussed in some more detail in the following.

(1) Sound absorption. Sound absorption is the attenuation due to shear viscosity (μ), bulk viscosity (μ_B) thermal conductivity (κ) and possible relaxation effects in the fluid [12]. The influence of absorption on the SNR is accounted for through the sound absorption coefficient α_{abs}, cf. Eq. (3). As an investigation of sound absorption in various oils of different viscosity, being used in flow testing of LUFMs, experimental measurements and calculations have been made for selected samples of such oil types, cf. Table 4. For reference of the measurement method, other oil types (castor oil and rapeseed oil) have also been included in the study, since published data for both viscosity and sound absorption are available for these oil types (which is seldom the case!). On castor oil the agreement with experimental and theoretical literature results [13-15] is better than 0.1 dB/cm over the complete frequency range investigated here (0.5 - 1.2 MHz). The measurements were made using a combined sound velocity / sound attenuation measurement cell developed in ref. [16], applying a modified measurement method. The measurements have been compared with calculations using the classical absorption coefficient (with no description of relaxation effects), given as

$$\alpha_c = \frac{\omega^2}{2\rho c^3}\left(\frac{4}{3}\mu + \mu_B + \frac{(\gamma-1)\kappa}{c_p}\right), \tag{4}$$

where $\omega = 2\pi f$ is the angular frequency, ρ is the fluid density, c is the sound velocity, γ is the ratio of specific heats, and c_p is the specific heat capacity. On lack of bulk viscosity data for the oil types investigated here, we have here used $\mu_B = (4/3)\mu$ as for lubrication oil [28]. The measurement and calculation results are shown over a broad frequency range in Fig. 2. Among these, the oil types of interest for LUFM operation are the five types given in Table 4 from "light oil" to "extra heavy oil". A fair agreement between the measurement results and the classical sound absorption coefficient is observed, for the oil types investigated here. This includes the level of absorption, as well as its frequency dependence. However, the measurements should only be taken as tentative results.

Table 4. Liquid samples used for measurement and calculation of the sound absorption coefficient. The density, sound velocity and viscosity data given in the table are also measured values. All data apply to 20 °C and 1 atm. (Note that the five types from "light oil" to "extra heavy oil" are among those used in flow testing of the new LUFM design described in Section 6.)

	Density	Sound velocity	Viscosity	Absorption coefficient @ 1 MHz [dB/cm]	
Sample	[kg/m^3]	[m/s]	[cP]	Measured	Calculated (α_c)
Water (destilled)	998	1480.0	-		
"Light oil"	809	1347.3	3	0.02	0.007
"Medium oil"	848	1401.5	11.5	0.07	0.02
"Brad Penn"	867	1422.1	16.5	0.04	0.03
"Heavy oil"	865	1441.3	48	0.09	0.09
"Extra heavy oil"	881	1480.0	297	0.45	0.48
Rapeseed oil	915	1470.4	63.5	0.07	0.10
Castor oil	962	1520.8	775	0.78	1.05

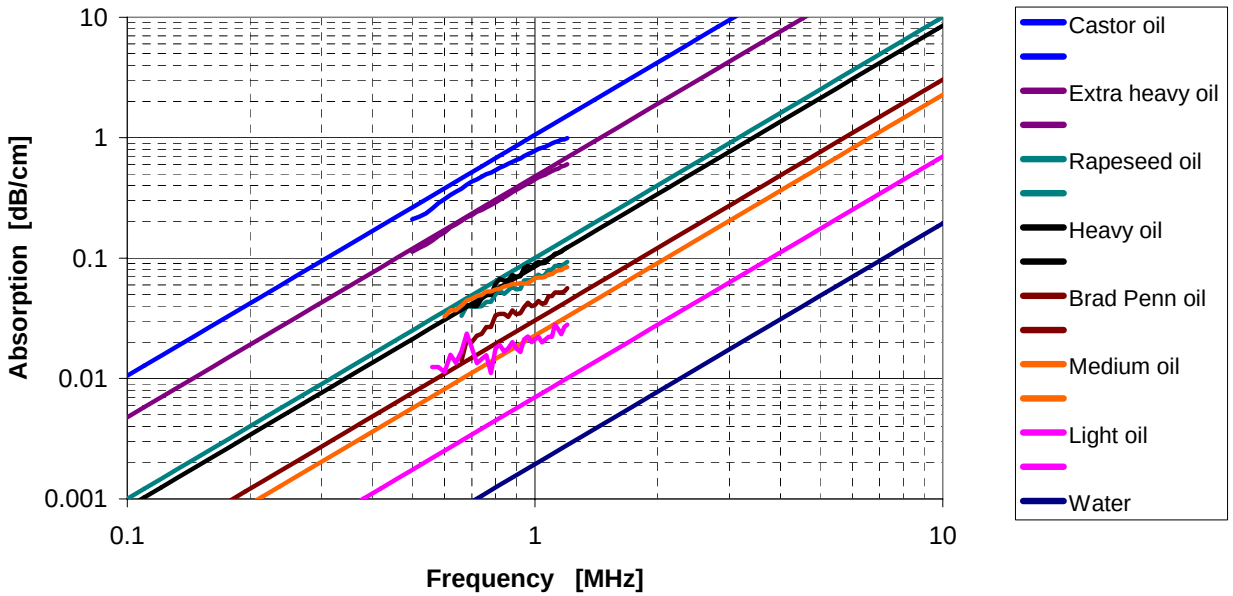

Fig. 2. Measured and calculated sound absorption coefficient α_{abs} for the liquid samples given in Table 4 (various oils and water), at 20 °C, shown as a function of frequency. The "non-straight" lines are measurement results, and the straight lines are calculated (classical absorption) results.

If we take 1 MHz as a typical operational frequency of current-day LUFMs, it is observed that four out of the five oil types (of interest for LUFM operation) investigated in Fig. 2 display sound absorption less than 0.1 dB/cm at 1 MHz. These fluids, with viscosity less than about 50 cP, should normally not represent problems for LUFMs less than e.g. 20" size, in this temperature range.

For "extra heavy oil", with viscosity 297 cP, however, the attenuation is higher, about 0.45 dB at 1 MHz, which means significant higher attenuation for large meters, relative to a low viscosity oil application. For 6" and 20" meters, that would correspond to about 10 dB and 32 dB increased attenuation, respectively, for centre paths. Especially for the 20" meter, this may be a significant attenuation and reduction of the SNR.

Excess absorption may be caused by relaxation effects, due to e.g. internal molecular vibrations, rotations, etc. The influence of relaxation on the SNR is accounted for in the attenuation coefficient α_{abs}, cf. Eq. (3). Such effects may cause significant excess absorption in the frequency band of the relaxation mechanism [12]. That means, at frequencies close to the relaxation time, τ (i.e. $\omega\tau \sim 1$), the energy loss per signal period is maximized. Relaxation effects will also express itself as dispersion (that the sound velocity varies with frequency). For LUFMs relaxation may cause significant extra attenuation if the relaxation frequencies of the oil in question is in the operational frequency band of the LUFM. Whether this is the case or not has to be investigated for the oil type at hand. For the oil types investigated here (Fig. 2) the measurements have not revealed any significant relaxation effects in the frequency band around 1 MHz.

(2) Water-in-oil (emulsion) effects. Water droplets in the oil cause excess sound attenuation due to scattering of the sound waves by the droplets. The excess effect on the SNR is accounted for through the attenuation coefficient α_{wio}, cf. Eq. (3). The major question is of course "how much water can be tolerated in the oil before the LUFM performance is significantly influenced?" Before such a question can be answered, one needs improved insight into which mechanisms that dominate the sound attenuation when water is present in the oil. Parameters of relevance in that context include the water droplet size distribution, the amount of water present in the oil, the pressure and temperature, the oil type (constituting the continuous phase), the LUFM signal frequency, etc. As an example, Fig. 3 shows simulations of the combined attenuation terms $\alpha_{abs}+\alpha_{wio}$ as a function of droplet diameter (over the range 0.1 μm to 10000 μm = 1 cm), for 5 % water-in-oil emulsions, at 1 atm. pressure and a frequency of 1 MHz, using the Waterman-Truell multiple scattering model [17-19][3].

[3] The present results are calculated using the Waterman-Truell multiple scattering model with Allegra-Hawley scattering coefficients [17-19]. This model takes into account the thermal and viscous boundary layer effects close to the droplet surface (inside and outside of the droplet), the generation of sound waves inside and outside of the droplets, and higher order oscillation modes (monopole, dipole, quadropole, etc.). The model is potentially applicable at all frequencies of relevance, from very long to very short acoustic wavelengths relative to the droplet diameter. This includes droplet resonances appearing when the acoustic wavelength is of the order of the droplet diameter.

The Waterman-Truell multiple scattering model for two-phase fluids has expressed good agreement with experimental measurements for a wide range of Exxsol D80-in-water and water-in-Exxsol D80 emulsions [16], and for aerosols (e.g. water droplets in air) [20]. Several other types of models for description of sound propagation in two-phase media have also been implemented and used extensively, for comparison and reference (not shown here).

Fig. 3a shows $\alpha_{abs}+\alpha_{wio}$ calculated for water droplets in the oil types given in Table 4, at 20 ^{o}C. Several important features are noted. Firstly, two dominant "peaks" are observed in $\alpha_{abs}+\alpha_{wio}$, the first one at droplet sizes of about 0.35 μm, the other one at sizes of about 5 mm and above. The first one is due to thermoviscous effects in a boundary layer around each droplet interface. The second one is due to scattering of sound by the droplet itself, i.e. an effect caused by the contrast in the acoustic impedance between the continuous oil phase and the water droplet. At these "peaks" the attenuation $\alpha_{abs}+\alpha_{wio}$ is relatively high, in the range of about 0.5 dB/cm and above. Inbetween the two "peaks" $\alpha_{abs}+\alpha_{wio}$ displays a "valley" with lower attenuation, since in this droplet size range there is no dominating attenuation mechanisms. By comparison with Fig. 2, it turns out that in the "valley", the attenuation is essentially dominated by α_{abs} (given by Fig. 2), and that the excess attenuation due to water-in-oil scattering, α_{wio}, is relatively small. Consequently, for the oil types investigated here and for the 5 % water concentration considered, the simulations indicate that high attenuation may be expected for water droplet sizes in a band below 1-2 μm and in a band above e.g. 2-3 mm (depending on oil type). However, for water droplets in the range of, say, 2 μm to 2 mm, the simulations indicate that the excess attenuation α_{wio} due to water-in-oil is negligible. For very small droplets, less than 0.1 μm, the simulations indicate that the excess attenuation α_{wio} due to water-in-oil becomes small.

It should be emphasized that the present example results are all based on simulations for a 5 % water-in-oil emulsion. For other water fractions the results are different, such as for "pipeline quality oil" (less than 1 % water, cf. Section 3), for which the attenuation will be smaller. However, a discussion of this matter is too large and complex to be covered in the present paper.

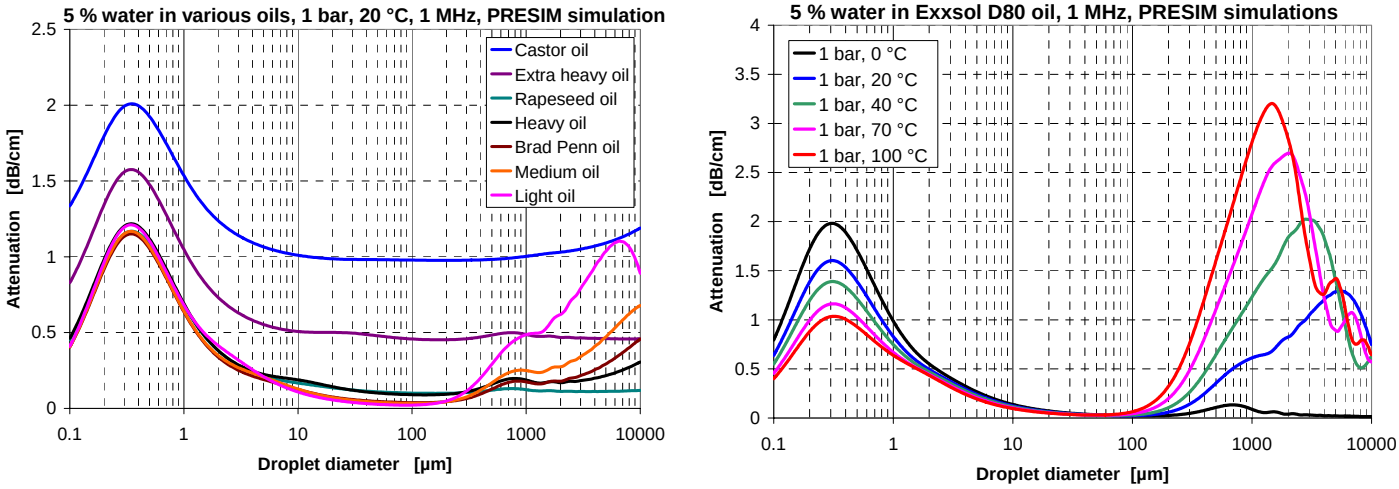

Fig. 3. Numerical calculations (using the Watermann-Truell multiple scattering model) of sound attenuation $\alpha_{abs}+\alpha_{wio}$ in 5 % water-in-oil emulsions, shown as a function of water droplet diameter, at 1 MHz. (a) Selected oils at 1 atm / 20 ^{o}C / 1 MHz (cf. Table 4), (b) Exxsol D80 model oil at 1 atm. and different temperatures in the range 0 to 100 ^{o}C

Additional simulation results (not shown here) indicate that the main characteristics of the results shown in Fig. 3a do not change much by lowering the frequency some hundred kHz, except that the overall level of the attenuation $\alpha_{abs}+\alpha_{wio}$ of course becomes smaller at these lower frequencies.

Additional simulation results (not shown here) also indicate that the influence of pressure on these results should not be large, as expected. The reason for that is of course the low compressibility of the fluids.

There is then the question of temperature influence. Unfortunately, relevant properties of the oil types given in Table 4 have not been sufficiently available to enable any simulation of temperature effects on $\alpha_{abs}+\alpha_{wio}$. On lack of better data, temperature effects were then simulated using the model oil Exxsol D80 as the continuous phase. Simulations of $\alpha_{abs}+\alpha_{wio}$ for 5 % water-in-Exxsol D80 at different temperatures in the range 0 to 100 ^{o}C are shown in Fig. 3b, at otherwise the same conditions as for Fig. 3a. It appears that temperature has a significant influence on the two attenuation "peaks" discussed above, but not so much inbetween the "peaks". The attenuation level of the "left peak" increases significantly at the lowest temperatures in this range, while for the "right peak" the attenuation level increases significantly at the highest temperatures, accompanied by a move of the "peak" towards lower droplet sizes. At these "peaks", the simulated attenuation levels are so high that, if they are correct, droplet sizes in these ranges would definitely have consequences for operation of LUFMs.

It is strongly emphasized here, that before being taken into use as any part of a basis for operation of LUFMs, attenuation results for water-in-oil such as those indicated by Fig. 3 through theoretical modelling, need to be experimentally verified, by measurements. Work has been started also on this experimental part (not shown here)[4].

(3) Gas-in-oil effects. Free gas (e.g. in the form of gas bubbles) in the oil causes excess sound attenuation due to scattering of the sound waves by the bubbles, bubble resoncances, etc. The excess effect on the SNR is accounted for through the attenuation coefficient α_{gas}, cf. Eq. (3). Again, the major question is "how much free gas can be tolerated in the oil before the LUFM performance is significantly influenced?" Parameters of relevance in that context include the bubble size distribution, the amount of free gas present in the oil, the pressure and temperature, the oil type (constituting the continuous phase), the LUFM signal frequency, etc. As an example, Fig. 4 shows simulations of the combined attenuation terms $\alpha_{abs}+\alpha_{gas}$ as a function of droplet diameter (over the range 0.1 μm to 10000 μm = 1 cm), in Exxsol D80 model oil with air bubbles, for different bubble concentrations (10 ppm to 1 %), at 20 ^{o}C and 1 MHz, using the Waterman-Truell multiple scattering model [17-19]. The attenuation $\alpha_{abs}+\alpha_{gas}$ is calculated for two pressures, 1 atm. and 100 bara, shown in Figs. 4a and 4b, respectively.

The 1 atm. results given in Fig. 4a are discussed first. This case is not of much practical interest, since operation at 1 atm. is normally not relevant for the LUFMs in question here, but may be of interest to illustrate the physical mechanisms involved. Several important main features are noted. At bubble sizes of about 5-6 μm the attenuation displays a distinct "peak" due a bubble resonance. At the bubble resonance the attenuation level is dramatically high. Below the bubble resonance, the attenuation level is reduced until it reaches a constant but high level (in the range of Rayleigh scattering). Above the bubble resonance the attenuation level is also gradually reduced, approaching the attenuation of the continuous oil phase, α_{abs}. This happens at very

[4] As mentioned in another footnote, fair agreement with measurements has been obtained using the Waterman-Truell model for oil-in-water and water-in-oil emulsions, but for a low-viscosity oil (Exxsol D80) [16], and for aerosols [20]. To which degree such agreement can be obtained also for water-in-oil emulsions based on high-viscosity oils, remains to see.

large bubble sizes, from 1 mm and upwards. The overall level of the attenuation increases of course by increasing amount of gas in the oil.

At 100 bara the situation is different, both qualitatively and quantitatively, cf. Fig. 4b. The higher pressure contributes to stiffen the bubbles so that the resonance and scattering effects are reduced, and the bubble size at which the bubble resonance occurs is increased, to about 70-80 μm. In addition, higher harmonics of the bubble resonance are observed, as sharp resonance peaks at larger bubble sizes. In addition, a broad resonance occurs at about 1 μm. The simulation results indicate, if they are correct, that sound transmission at such pressures should not be a problem at low bubble concentrations, less than e.g. 100 ppm, except for a band in the vicinity of the bubble resonance. Transmission problems arise however at higher bubble concentrations. For a concentration of e.g. 1000 ppm = 0.1 %, the attenuation may be critically high except for bubble sizes larger than about 0.1-1 mm (depends on pipe diameter). For 10000 ppm = 1 %, the attenuation may be critically high except for bubble sizes larger than about 1-10 mm (depends on pipe diameter).

Note that the calculations shown in Fig. 4 have been made for monosize bubbles, evenly distributed in the oil. They thus represent "worst case" scenarios. Similar calculations made for bubble size distributions (not included here) show that the resonances are then "smeared out", accompanied by a reduction of the attenuation level.

The results shown in Fig. 4 apply to a frequency of 1 MHz. Additional simulations (not shown here) indicate that the attenuation due to gas bubbles decreases if the frequency is lowered, and that the bubble resonance moves slightly towards the region of larger bubbles.

The results shown in Fig. 4 apply to air bubbles in Exxsol D80 model oil. Bubbles of natural gas instead of air may give slightly higher attenuation, due to the lower density of natural gas (at otherwise equal pressure and temperature conditions). On the other hand, higher viscosity oil may decrease the attenuation, especially at the bubble resonances.

Additional simulations (at 70 ^{o}C, not shown here) also indicate that the influence of temperature on the results shown here may not be a dominating effect.

(a)

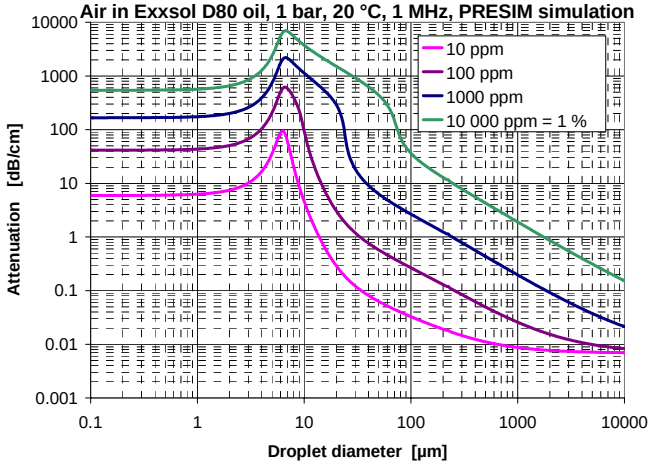

(b)

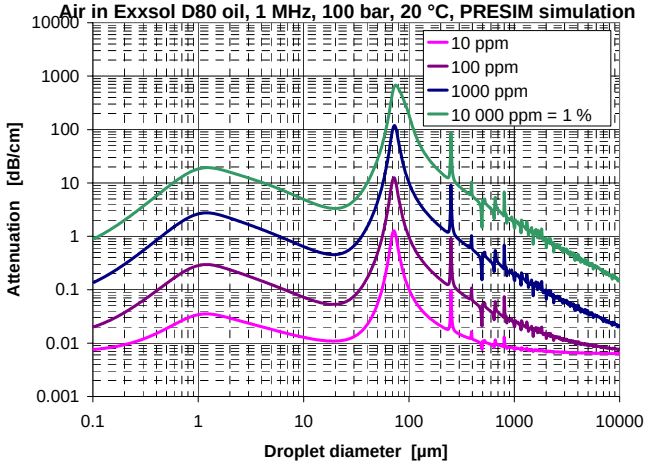

Fig. 4. Numerical calculations (using the Watermann-Truell multiple scattering model) of sound attenuation $\alpha_{abs}+\alpha_{gas}$ in Exxsol D80 model oil with air bubbles, shown as a function of bubble diameter, for different bubble concentrations (10 ppm to 1 %), at 20 ^{o}C and 1 MHz. (a) 1 atm. pressure, (b) 100 bara pressure.

(6) Solid-particles-in-oil (suspension) effects. Wax particles may be present in the oil it if the temperature is below the cloud point (cf. Section 3). Solid particles in the oil causes excess sound attenuation due to scattering of the sound waves by the particles. The excess effect on the SNR is accounted for through the attenuation coefficient α_{solids}, cf. Eq. (3). Again, the major question is "how much solid particles can be tolerated in the oil before the LUFM performance is significantly influenced?" Parameters of relevance in that context include the particle size distribution, the amount of particles present in the oil, the pressure and temperature, the oil type (constituting the continuous phase), the LUFM signal frequency, etc. Before a qualified answer to this question can be given, experimental measurements and numerical simulations using a scattering model accounting for solid particles[5] are needed to improve current-day knowledge on such effects, both qualitatively and quantitatively.

(4) Wax effects (contamination). Wax may also cause other effects. If the temperature is below the cloud point, wax contamination may build up at different surfaces of the LUFM. Possible influences which may be important for the LUFM performance include:

(a) Wax layer build-up at the transducer fronts. Such build-up may shift the transit times and cause a continuous meter factor shift as the wax builds up. For example, a 0.1 mm wax layer on all transducer fronts would result in a systematic meter factor shift of about 0.08 and 0.03 % for a 6" and a 20" flow meter, respectively. Regular in-situ proving of the flow meter will however correct for such misreading.

Wax build-up may also cause excess attenuation and contribute to reduce the SNR. However, due to the relatively small difference in the acoustic impedance between oil and wax, a thin wax layer may not be expected to affect the SNR significantly, unless the layer becomes thick, and if inhomogeneities are present. The excess effect on the SNR is accounted for through the attenuation coefficient α_{wax}, cf. Eq. (3).

(b) Wax build-up in the transducer cavities, at the sides of the transducer. Such build-up may cause reduced acoustic isolation of the transducer from the spoolpiece, with increased level of acoustic "cross-talk" through the spoolpiece as a result. Since such cross-talk acts as coherent noise, this results in reduced SNR, and thus reduced accuracy of the transit time measurements.

(c) Wax build-up on the inner wall surface of the spoolpiece (in the pipe bore itself). Such wax build-up results in a deviation between the actual cross-sectional area seen by the liquid flow and the "supposed" area (i.e. the area in case of no wax present). The consequence is incorrect volumetric flow rate reading, and a systematic shift of the meter factor. The question is of course again; "how much wax build-up can be tolerated at the spoolpiece wall before the meter factor of the LUFM is significantly shifted?" A simple analysis reveals that for a thin wax layer distributed uniformly along the spoolpiece wall with effective thickness L, the relative change in cross-sectional area is given approximately as $\Delta A/A \approx 2L/R$, where R is the pipe radius and $A = \pi R^2$ is the cross-sectional area with no wax present. For a 6" flow meter, thus, a wax layer of 0.1 mm thickness will result in a misreading of 0.27 %, which is a large error, if not discovered and corrected for. For a 20" meter, the misreading is proportionally smaller, about 0.08 %. Such

[5] That means, accounting for both compressional and shear waves in the particle, not only compressional waves, such as the Waterman-Truell model [17-19] used for fluids here.

wax build-up at the spoolpiece wall may be difficult to discover in-situ, although methods for in-situ wax build-up detection may be available. Regular in-situ proving of the flow meter will however correct for misreading due to such wax build-up.

4.2 Flow profiles, numerical integration and VPC

A combination of multipath configuration and numerical integration is necessary in UFMs to achieve sufficient measurement accuracy in cases of disturbed flow velocity profiles. The lateral chord positions y_i and integration weights w_i , $i = 1,..., N,$ (cf. Eq. (1)) are chosen to account for e.g.

- Robustness and accuracy with respect to disturbed (asymmetric) axial flow velocity profiles.
- Compensation for transverse (non-axial) flow components (swirl, cross-flow, etc.).
- Effects of orientation of the meter relative to the flow profiles.
- Reynolds number dependency.
- Pipe roughness effects (influencing on flow profiles).

Although the integration method in actual UFMs may display a high degree of robustness to installation conditions (bends, flow conditioners, etc.) using constant integration weights w_i, there is one effect which needs special treatment: the "velocity profile effect". This effect and its treatment is addressed in the following.

The essence of the "velocity profile effect" experienced in UFMs is that numerical integration using constant integration weights w_i does not in general appear to be sufficient over the complete range of flow velocity profiles experienced at various Reynolds numbers, not even for the ideal situation of a straight pipe run with a very long upstream length. If constant integration weights were used, a distinct "nonlinearity" would appear in the flow calibration curve of the UFM. This effect means that there in some cases could be problems in meeting the linearity requirements of the UFM using such weights, and that special treatment is needed to avoid or reduce this effect.

The effect can be explained as follows. For convenience and without loss of generality[6], consider an example of a UFM with an even number of paths, e.g. $N = 4$. For symmetric flow profiles (e.g. such as expected in straight pipes with long upstream lengths) one then has, from Eq. (1),

$$\bar{v}_A = \sum_{i=1}^{4} w_i \bar{v}_i = 2\sum_{i=1}^{2} w_i \bar{v}_i \,, \tag{5}$$

where

$$\bar{v}_i = \int_{Path\ i} v_{A,i} d\ell \,, \qquad v_{A,i} = v_A(x, y = y_i, z, t) \,. \tag{6}$$

$v_A(x, y, z, t)$ is the axial flow velocity component in the position (x, y, z) at time t. $v_{A,i}$ is thus the value of v_A at the lateral chord position no. i. From Eq. (5) it follows that if the condition

[6] For USMs with odd number of paths, one path will normally be a centre path, and the arguments given in the text (for even number of paths) are not altered.

$$2\frac{w_1\bar{v}_1 + w_2\bar{v}_2}{\bar{v}_A} = 1 \qquad \Leftrightarrow \qquad w_1\left(\frac{\bar{v}_1}{\bar{v}_A}\right) + w_2\left(\frac{\bar{v}_2}{\bar{v}_A}\right) = \frac{1}{2}, \tag{7}$$

was fulfilled for all flow velocity profiles, the UFM would display perfect linearity (in case of symmetric flow profiles considered as an illustration here). In practice, this will not be the case if constant integration weights w_i are used. The weights w_i can be designed so that Eq. (7) is fulfilled for a certain flow velocity profile, but as the flow profile changes (e.g. with changing Reynolds number), it appears that Eq. (7) can not be fulfilled for all profiles, without changing the weights. Alternatively, one can use constant integration weigths and correct these afterwards, depending on the measured flow velocity profile. The latter technique is employed here and denoted "velocity profile correction" (VPC) [21].

The following example can illustrate this situation. Fig. 5a shows a number of symmetrical and experimental flow velocity profiles, measured as a function of relative lateral chord position y_i/R in straight pipe runs, most of them with long upstream lengths. The profiles have been normalized to the average axial flow velocity, $\bar{v}_A$, to give $v_{A,i}/\bar{v}_A$. Most of these flow velocity profile data (in the Reynolds number range 7000 - 10^7) are taken from published literature [22-26], supplemented with some own measurements at lower Reynolds numbers (Re = 1000 - 32000). In addition, the parabolic profile representing laminar flow has been included in the figure. Note that the lateral resolution in the latter data sets (the own measurements) is significantly courser than for the published literature data.

(a)

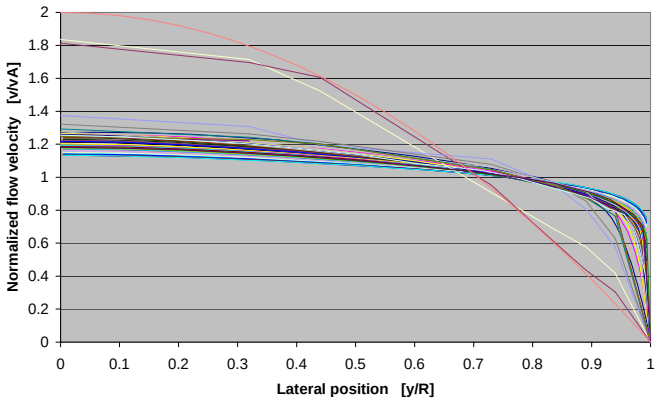

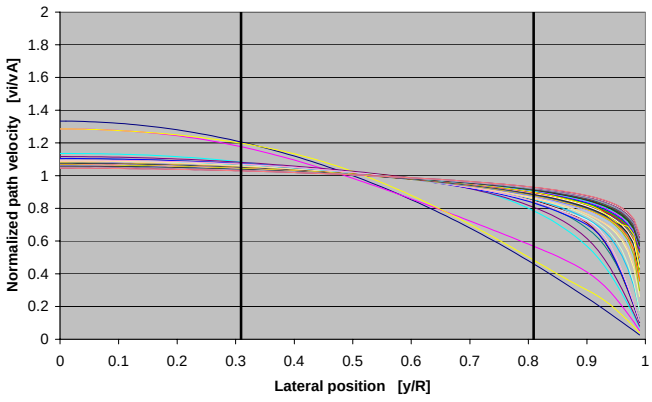

(b)

Fig. 5. (a) Normalized experimental flow velocity profiles, $v_{A,i}/\bar{v}_A$, measured in straight pipe runs, most of them with long upstream length. (b) Integrated (using Eq. (6)) and normalized experimental "flow velocity profiles", $\bar{v}_i/\bar{v}_A$.

In Fig. 5b the experimental flow velocity profiles given in Fig. 5a have been integrated over the relevant UFM paths, using the line integral, Eq. (6), and then normalized to $\bar{v}_A$. Consequently, the figure shows the ratio $\bar{v}_i/\bar{v}_A$ for the various profiles given in Fig. 5a, as a function of relative lateral chord position in the pipe, y_i/R. In Fig. 5b two vertical lines are also indicated. These are the relative lateral chord positions of the paths in a UFM configured with 4 paths in an

"asymmetric criss-cross" pattern ($\phi_i = \pm 45^o$), using the Gauss-Jacobi integration method (y_i/R = 0.3090 and 0.8090)[7].

At the position of these two vertical lines, the two ratios $\bar{v}_1/\bar{v}_A$ and $\bar{v}_2/\bar{v}_A$ are thus determined. These are the two ratios needed in Eq. (7). As can be seen from Fig. 5b, these two ratios overestimate and underestimate the flow, respectively. From Fig. 5b it is also seen that for the lateral chord positions used as an example here (cf. above), the first ratio, $\bar{v}_1/\bar{v}_A$, varies considerably less over the range of profiles than the second ratio, $\bar{v}_2/\bar{v}_A$, does. Consequently, when these ratios are multiplied with their respective integration weights, w_1 and w_2, and then added, according to Eq. (7), and if the integration weights are constant, it is evident that this sum is not a constant (and equal to ½) over the range of flow velocity profiles, as would be required by Eq. (7) for a completely linear UFM calibration curve. That means, the sum may be equal to ½ for some profiles, and different from ½ for others.

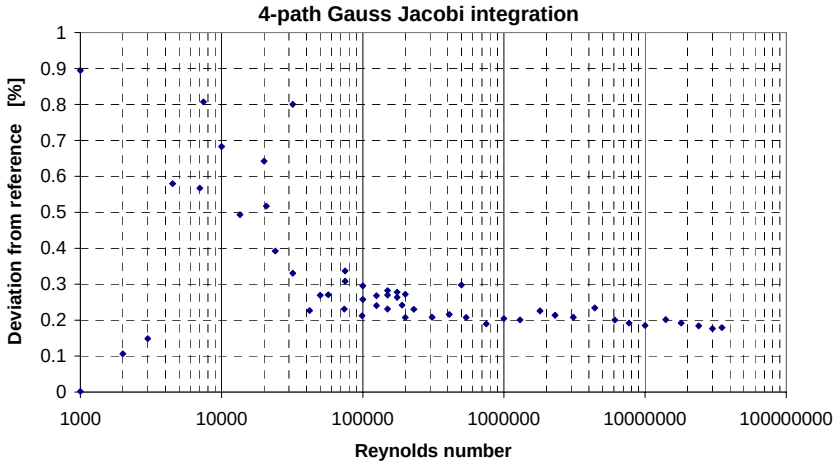

Fig. 6. "Linearity curve" for the illustration example of a 4-path UFM employing Gauss-Jacobi integration, for the "straight-pipe" experimental flow velocity profiles shown in Fig. 5, before applying any VPC.

Fig. 6 shows how this effect turns out for the 4-path Gauss-Jacobi integration method used as an example here, i.e. for the UFM measurement. At high Reynolds numbers, with fully developed turbulent flow, and relatively flat flow velocity profiles which do not change much (cf. Fig. 5), the UFM displays a fair degree of linearity (i.e. the deviation from reference is relatively constant). For Reynolds numbers of 10^5 and below, where the flow profiles are different, the deviation "curve" increases significantly (i.e. the measurement error increases), for the reasons explained above. At Reynolds numbers below about 7000 the deviation "curve" decreases. In essence, thus, for this integration method, there appears to be a distinct "bump" in the linearity curve.

Since the effect is basically due to the flow velocity profiles, this "velocity profile effect" is universal, and will be present in any UFM integration method employing constant weights. However, as can be seen from Fig. 5b and the above explanation, the actual form of the "bump" in the linearity curve will be different for different UFM integration methods (depending on the relative lateral chord positions y_i/R and the weights w_i used). The LUFM described and used in the present work (cf. Section 6) is based on a different integration method than this 4-path

[7] The Gauss-Jacobi integration method is used as a convenient example here, since it is a well-known and well documented integration method, which has also been used as integration method in gas and liquid UFMs.

Gauss-Jacobi integration (which has been used only as an example above, to explain the effect qualitatively).

In the LUFM used in Section 6, the "velocity profile effect" is compensated by employing a "velocity profile correction" technique, VPC [21], involving non-constant integration weights. Improvements achieved using VPC are illustrated in Section 6, cf. Fig. 8 showing LUFM measurement results after use of VPC.

In connection with crude oil operation, an important question is how the "velocity profile effect" and the associated "bumb" will be influenced by the fluid quality. It turns out that since the flow velocity profile depends on Reynolds number, viscosity is the fluid quality parameter of importance in this respect. Increasing viscosity means decreasing Reynolds number and reduced flatness of the flow velocity profiles. Flow velocity profiles relevant for different viscosities, as well as asymmetries in the flow profiles, are taken into account in the VPC method [21].

5. API STANDARD AND PROVING ISSUES

Proving liquid ultrasonic meters is similar to other meters, but because of the sampling methods employed they produce a greater degree of data scatter. API, in developing the ultrasonic meter standard [1] understood these differences, and recommend methods to successfully prove these meters. This section outlines the accuracy requirements, the unique problems with proving ultrasonic meters, the recommendations for proving, and need for in-situ proving.

5.1. Meter accuracy requirements and criteria

Accuracy requirements for the wholesale and retail trade are normally defined by the weights and measures regulations in the country or jurisdiction in which the sale is conducted. Sales within the petroleum industry that are not normally defined by weights & measures, but by a contract between the trading parties, are known as Custody Transfer transactions. A typical contract may define a specific measurement standard such as one of the American Petroleum Industry (API) Standards. Currently API recognizes four types of dynamic measuring devices: (a) Positive Displacement (PD) Meters, (b) Turbine Meters, (c) Coriolis Mass Flow Meters (CMFMs) and (d) recently approved Liquid Ultrasonic Flow Meters (LUFMs). The API Standards are based on best practice and define the proper application of a specific flow meter. Contracts are also based on other recognized standards but all these standards have one thing in common - they all strive to minimize measurement error for a specific application.

The API Standard for LUFMs [1] is specifically written for custody transfer measurement but also addresses other applications such as allocation measurement, check meter measurement, and leak detection measurement.

It states that the meter factor shall be determined by proving the meter at stable operating conditions, (i.e., essentially constant: flow rate, density, viscosity, temperature, and pressure). Since the essential purpose of proving is to confirm the meter's performance at normal operating conditions, in-situ proving is preferred because it eliminates installation and operating effects which can affect a meter's accuracy and repeatability.

5.2. Proving liquid ultrasonic flow meters

Field proving of liquid ultrasonic flow meters is difficult for two reasons:

1. The UFM output pulses are not related in "real time" to the meter through-put. There is a time delay between what is being measured and the pulse output. Reducing the meter's response time and / or increasing the prover volume are recommended.

2. The inertia free measuring principle makes the UFMs far more "sensitive" to operating conditions than conventional meters (turbine and PDs), in the sense that UFMs can follow rapid changes (fluctuations) in the flow. This is normally an advantage, but in *proving* the UFM it may be a disadvantage. The measurement accuracy is improved by taking more samples and / or using a larger prover.

The API Ultrasonic Flow Meter Measurement standard [1] provides suggested prover volumes and the number of runs to achieve custody transfer accuracy.

Typically custody transfer accuracy requires a repeatability of 0.05 % in 5 consecutive prover runs. Since repeatability, by definition, is at constant conditions, the uncertainty of the measurement is due to random errors. Statistically, a repeatability of 0.05 % in 5 runs is equivalent to ± 0.027 % uncertainty at 95 % confidence level. This same level of uncertainty can be met by using more or less repeatability runs. Table 5 gives an abbreviated overview of the number of runs and repeatability required to achieve the stated level of uncertainty. The table is taken from [1] and was derived from [27].

Table 5. Proving an ultrasonic liquid flow meter (from [1], Table B-1).

No. of repeatability proving runs	Repeatability*	Uncertainty (95 % conf. lev.)
3	0.02 %	0.027 %
5	0.05 %	0.027 %
10	0.12 %	0.027 %
15	0.17 %	0.027 %
20	0.22 %	0.027 %

* Per API MPMS, Ch. 4.8, Table A-1 to achieve 0.027 % uncertainty of meter factor

Table 6. Prover volume vs. meter size, for turbine meters (TM) vs. ultrasonic meters (LUFM), to achieve ± 0.027 % uncertainty of meter factor (95% conf. level).

Prover Volume vs. Meter Size				
	5 runs 0.05 %		8 runs 0.09 %	10 runs 0.12 %
	Prover Size (barrels)			
Meter Size	Turbine Meters	Ultrasonic Meters*		
4”	5	33	15	10
6”	12	73	34	22
8”	20	130	60	40
10”	24	203	94	62
12”	48	293	135	89
16”	100	521	241	158

* Per API MPMS, Ch. 5.8 [1] (Table B-2)

For ultrasonic meters the prover volume should also be increased to insure acceptable results. Table 6 provides a comparison between typical prover volumes for turbine meters at 5 repeatability runs, and the same size ultrasonic meter at 5,8 and 10 repeatability runs, to achieve ± 0.027 % uncertainty at 95% confidence level. The ultrasonic meter numbers are taken from ref. [1].

To better handle the random uncertainty, and improve the repeatability of an ultrasonic meter "groups" proving can be used. This method is outline in API MPMS 4.8 "Operation of proving Systems". It states that "The scatter in erratic meter proving data can be normalized by averaging the results of several meter proving runs and comparing the average of these small sets for agreement with the deviation limits." This method was employed in the lab testing of ultrasonic meters by running 14 consecutive runs, eliminating the first 3 to insure stable conditions, and grouping the remaining 11 runs into 5 groups of 7 runs each. The method makes use of all the data and provides significantly better results.

5.3. The need for proving

Validation, proving, a meter is always import for measurement certainty. For ultrasonic meters there are two methods that can be used: (1) In-situ testing in the field under operating conditions, or (2) lab testing under simulated conditions. The method employed depends on the amount of uncertainty that is acceptable. Meters used in the wholesale and retail sales almost universally require in-situ proving. The custody transfer of petroleum products by contract also almost always stipulate onsite proving.

Other applications may use meter factors established in a laboratory, but the measurement uncertainty increases. The installation effects are very difficult to asses quantitatively because of the many different configurations of piping, combined with the effect of in-line accessories like valves and strainers.

Influences of fluid properties on UFM performance have been pointed out and discussed to some extent in Section 4. For example, the presence of water droplets, gas bubbles or wax particles in the oil may cause significantly increased sound attenuation, cf. Figs. 3 and 4. For high-viscosity oils the sound absorption of the oil itself may also be significant. If so, the result may be a degraded signal-to-noise ratio (SNR).

Degradation of the SNR will lead to degradation of the accuracy of the LUFM. In many cases the SNR will not be the same in the in-situ field operation as it was in a factory flow calibration situation. Possible errors should therefore be measured and accounted for in both places, such as by in-situ proving of the LUFM.

Regular in-situ proving of the LUFM will also correct for possible misreading (shift in the meter factor) due to possible build-up of wax at (a) the transducer fronts, and (b) the spool piece wall.

Before better and more quantitative knowledge is available on how UFMs react to different fluids, the arguments advocating reduced need for in-situ proving and increased dependency on laboratory flow calibration (e.g. using water instead of hydrocarbons) [10,11], are highly questionable.

6. DEVELOPMENT RESULTS

The present project has lead to the development of a 6 path liquid ultrasonic flow meter which will be commercialized as Smith Meter™ Ultra[6].

The meter has been developed for the high accuracy measurement of refined petroleum products and crude oils. The main design criteria for the Ultra[6] were to develop a meter that could provide both high reliability and measusment stability in a wide range of petroleum applications. Since most petroleum applications are in harsh outside environments the packaging of the electronics is especially important. Measusment stability, as seen from this paper, depends on the proper application of the meter as well as the operation of the meter. The Ultra[6] has been built with experience in these applications and provides another measurement instrument for the industry. Application is so highly tied to performance that it always key to accurate measusment.

Significant synergies have been achieved, in several respects, between FMC Kongsberg Metering's MPU 1200, 600 and 200 gas ultrasonic flow meters [29], and FMC Smith Meter's Ultra[6] liquid ultrasonic flow meter. This relates to development synergies (cf. e.g. [30]) as well as production synergies.

The product line for the Ultra[6] will be released worldwide in phases for application on 6” - 20” lines and flow rates to 7500 m^3/h.

Fig. 7. 8” Smith Meter™ Ultra[6] Liquid Flowmeter with Signal Process Unit (SPU).

The meter has been tested over a wide range of operation conditions, with and without the patented VPC method [21] (software only). Typical results for an 8" meter on 2 cSt and 30 cSt products are shown in Fig. 8. The linearity is within ± 0.115 % and ± 0.161 %, respectively, over a 10.5:1 turndown ratio, for the two examples shown here.

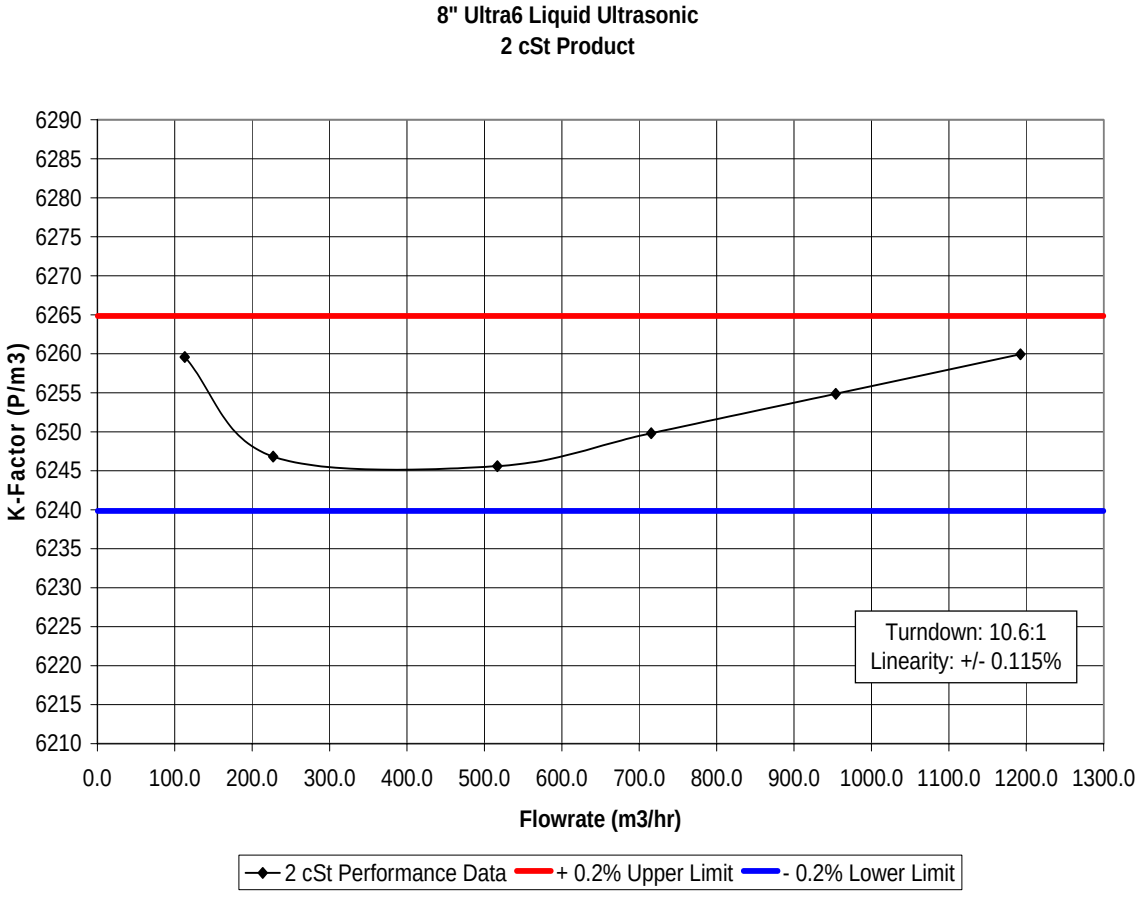

(a)

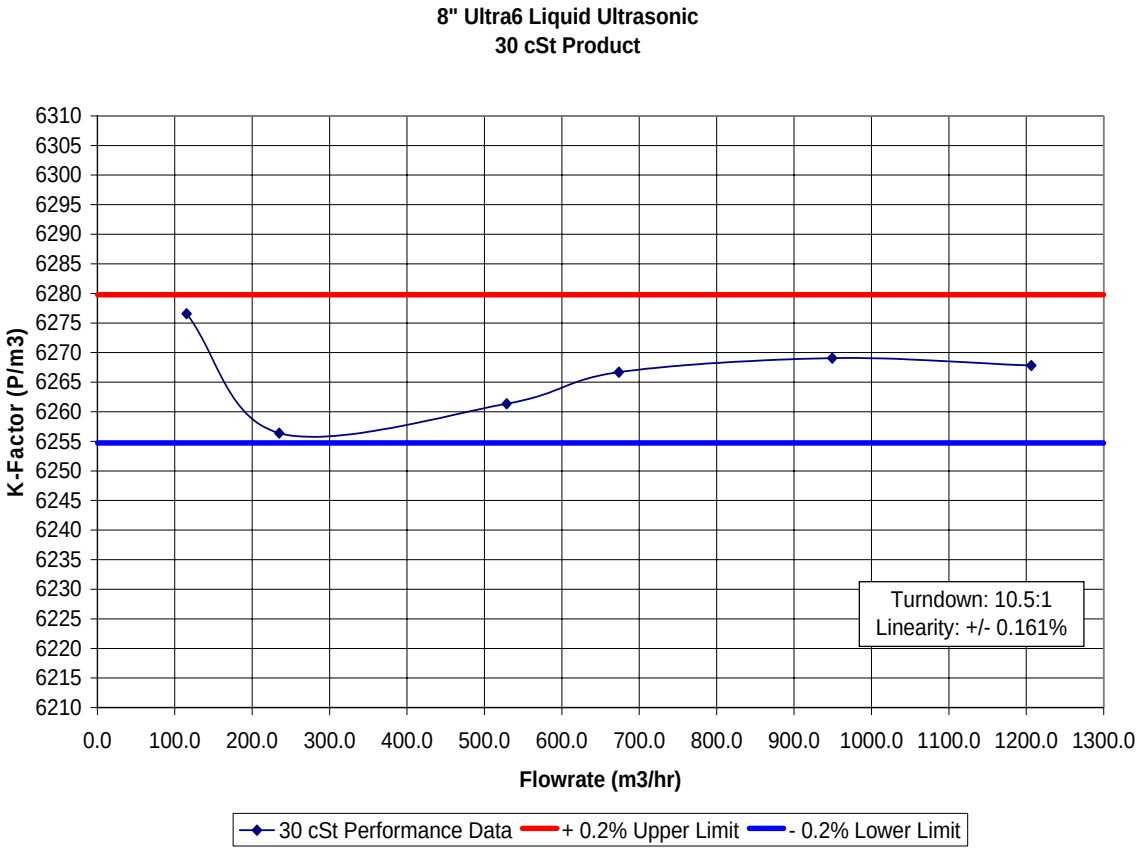

(b)

Fig. 8. Typical test results for an 8" Smith Meter™ Ultra[6] Liquid Flowmeter, on (a) 2 cSt and (b) 30 cSt products.

7. CONCLUSIONS

The advantages of ultrasonic meters make them well suited choice for high volume applications such as pipelines and ship loading / unloading facilities. Like turbine meters they are best operated at the higher flow ranges for optimum accuracy, but with techniques such as VPC, accurate measurement also at the lower flow ranges can be achieved. No pressure loss reduces operating cost. No moving parts increases service life and may reduce the frequency of proving, because usage wear is a key reason why meters are recalibrated.

The measurement technique is susceptible to installation effects and fluid properties. As with all meters, LUFMs need to be proven. In-situ proving, even though difficult, is indisputably the best method to reduce the total measurement uncertainty. Proving the meters in a laboratory offers an alternative, but at substantially higher risk of measurement error. Even though a specific ultrasonic meter may compensate for installation effects such as swirl or cross flow, there isn't any means of verifying this without field proving. The measurement accuracy is further compromised by the fluid property effects that were discussed in this paper. This is especially true for crude oils, because their properties are difficult to simulate even in a laboratory that tests with hydrocarbon fluids. Before better and more quantitative knowledge is available on how LUFMs react on different fluids, the arguments advocating reduced need for in-situ proving and

increased dependency on laboratory flow calibration (e.g. using water instead of hydrocarbons), are highly questionable.

Ultrasonic meters can provide accurate measurement over a wide range of crude oil applications if they are properly applied, proven and operated.

ACKNOWLEDGEMENTS

Significant technical contributions to the present work has been provided by the ULTRA[6] development team, consisting of (in addition to the authors) Kjell-Eivind Frøysa, Reidar Bø, Remi Kippersund and Stig Heggstad, Christian Michelsen Research AS, Norway; Skule Smørgrav, Atle K. Abrahamsen and Tom Heistad, FMC Kongsberg Meterering, Norway; Dave Resch, Jim Breter, Bob Smith and Joshua Rose, FMC Measurement Solutions, U.S.A.; and Magne Vestrheim, University of Bergen, Norway. The work has been supported by The Research Council of Norway (NFR).

REFERENCES

[1] **API MPMS Ch. 5.8,** "Manual of petroleum measurement standards, Chapter 5 - Metering, Section 8 - Measurement of liquid hydrocarbons by ultrasonic flow meters using transit time technology", 1st edition, American Petroleum Institute (API), Washington DC, U.S.A (February 2005).

[2] **AGA-9**, "Measurement of gas by ultrasonic meters", A.G.A. Report no. 9, American Gas Association, Transmission Measurement Committee (June 1998). (Revision in preparation.)

[3] **ISO/CD 18089 Part 1**, "Measurement of flow in closed conduits – ultrasonic meters for gas; meters for custody transfer and allocation measurement", International Organization for Standardization, Geneve, Switzerland (April 2005). (Committee draft standard only.)

[4] **Lunde, P., Frøysa, K.-E. and Vestrheim, M. (eds.),** "GERG project on ultrasonic gas flow meters, Phase II", GERG TM11 2000, Groupe Européen de Recherches Gazières (VDI Verlag, Düsseldorf, 2000).

[5] **Lunde, P. and Frøysa, K.-E.,** "Handbook of uncertainty calculations - Ultrasonic fiscal gas metering stations", Norwegian Petroleum Directorate, Norwegian Society for Oil and Gas Measurement (NFOGM), Christian Michelsen Research, Norway (December 2001). ISBN 82-566-1009-3 (free download available on web site www.nfogm.no).

[6] **Lunde, P., Frøysa, K.-E., Neumann, S. and Halvorsen, E.,** "Handbook of uncertainty calculations. Ultrasonic fiscal gas metering stations". *Proc. of 20th North Sea Flow Measurement Workshop,* St. Andrews Bay, Scotland, 22-25 October 2002.

[7] **Poynter, W. G.,** "Fundamentals of Liquid Measurement – Part 1", *Proc. of 76th ISHM (2001)*, p. 186.

[8] **Spitzer, D.,** "Industrial Flow Measurement", ISA (1990).

[9] **Miller, R. W.,** *Flow Measurement Engineering*, 3rd edition (McGraw-Hill, 1996).

[10] **Estrada, H., Cousins, T. and Augenstein, D.,** "Installation effects and diagnostic interpretation using the Caldon ultrasonic meter", *Proc. of 22nd North Sea Flow Measurement Workshop,* St. Andrews Bay, Scotland, 26-29 October 2004.

[11] **Hogendoorn, J., Laan, D., Hofstede, H. and Danen, H.,** "Altosonic III – A dedicated three-beam ultrasonic flowmeter for custody transfer of liquid hydrocarbons", *Proc. of 22nd North Sea Flow Measurement Workshop,* St. Andrews Bay, Scotland, 26-29 October 2004.

[12] **Kinsler, L. E., Frey, A. R., Coppens, A. B. and Sanders, J. V.,** *Fundamentals of Acoustics*, 4th edition (J. Wiley & Sons, New York, 2000).

[13] **D. Shore, M.O. Woods and C.A. Miles,** "Attenuation of ultrasound in post rigor bovine skeletal muscle", Ultrasonics, 81-87 (March 1986).

[14] **M. Freese and D. Makow,** "High-Frequency Ultrasonic Properties of Freshwater Fish Tissue", J. Acoust. Soc. Amer., **44**(5), 1282-1289 (1968).

[15] **Ping He,** "Acoustic parameter estimation based on attenuation and dispersion measurements", *Proc. of 20th Annual International Conference IEEE/EMBS, Oct. 29 - Nov. 1, 1998, Hong Kong.*

[16] **Ø. Nesse,** "Sound propagation in emulsions", Dr. Scient (Ph.D.) thesis, University of Bergen, Dept. of Physics, Bergen, Norway (January 1998).
[17] **Waterman, P. C. and Truell, R.,** "Multiple scattering of waves", J. Math. Phys. **2**, 512-537 (1961).
[18] **Frøysa, K.-E.:** "Separator instrumentation. A User Documentation of PRESIM 1.0", CMR Report CMR-93-F10011 (August 1993). (Confidential.)
[19] **Allegra, J. R. and Hawley, S. A.:** "Attenuation of Sound in Suspensions and Emulsions: Theory and Experiments", J. Acoust. Soc. Am. **51**, 1545-1564 (1972).
[20] **Lunde, P., Frøysa, K.-E., Fossdal, J. B. and Heistad, T.:** "Functional enhancements within ultrasonic gas flow measurement", Proc. of the *17th International North Sea Flow Measurement Workshop*, Oslo, Norway, 25-28 October 1999.
[21] **Frøysa, K.-E., Lunde, P. and Kalivoda, R.,** "Ultrasonic flow meter with velocity profile correction", US Provisional Patent Application No. 12878, Filed December 8, 2004.
[22] **Laufer, J.,** "The structure of turbulence in fully developed pipe flow", NBS Report No. 1174, National Bureau of Standards, USA (1952).
[23] **Dürst, F., Jovanovic, J. and Sender, J.,** "LDA measurements in the near-wall region of a turbulent pipe flow", J. Fluid Mech., **295**, 305-335 (1995).
[24] **Zagarola, M. and Smits, A.,** "Experiments in high Reynolds number turbulent pipe flow ", Phys. Rev. Lett., **78**(2), 239-242 (1997).
[25] **Perry, A. E., Henbest, S. M. and Chong, M. S.,** "A theoretical and experimental study of wall turbulence", *J. Fluid. Mech.* **165**, 163-199 (1986).
[26] **den Toonder, J. M. J.,** "Drag reduction by polymer additives in a turbulent pipe flow: laboratory and numerical results", PhD thesis, Delft University of Technology, The Netherlands (1995).
[27] **API MPMS,** Section 4.8 "Operation of Proving Systems" and **API,** Ch. 13.1 "Statistical Concepts and Procedures in Measurement", American Petroleum Institute (API), Washington DC, U.S.A.
[28] **Tasköprülü, N. S., Barlow, A. J. and Lamb, J.,** "Ultrasonic and visco-elastic relaxation in lubricating oil", J. Acoust. Soc. Am., **33**, 278-285 (1961).
[29] "Ultrasonic gas flow meter MPU 1200. Specifications", Bulletin SSKS001, Issue/Rev. 04 (5/02), FMC Measurement Solutions (2005). Web page: http://info.smithmeter.com/literature/docs/ssks001.pdf
[30] **Lunde, P., Vestrheim, M., Bø, M., Smørgrav, S. and Abrahamsen, A**, "Reciprocity and its utilization in ultrasonic flow meters", *Proc. of 23rd Intern. North Sea Flow Measurem. Workshop, Tønsberg, Norway, 18-21 October 2005*.